Lecture note at *Czech Technical University in Prague* **September 4 and 6, 2006**

Introduction to an area-preserving crystalline curvature flow equation*

Shigetoshi YAZAKI†

Abstract

I'm going to talk how to derive crystalline curvature flow equation as a gradient flow of total interfacial energy with the singular anisotropy. The talk will be focused on the basic part of the following topics:

- evolution of plane curves
- anisotropy / the Wulff shape, etc.
- crystalline curvature flow equation and its area-preserving version

Key Words: evolving interfaces, polygonal curves, curvature, curve-shortening, crystalline curvature, anisotropy, the Frank diagram, the Wulff shape, admissibility, area-preserving

Contents

*This short note is the lecture note for a seminar which is held while the author is visiting Czech Republic within the period from August 18 to September 19, 2006; this visit is sponsored by Czech Technical University in Prague, Faculty of Nuclear Sciences and Physical Engineering within the Jindřich Nečas Center for Mathematical Modelling (Project of the Czech Ministry of Education, Youth and Sports LC 06052). A part of research in this note is/was supported by Grant-in-Aid for Encouragement of Young Scientists No. 17740063.

†Faculty of Engineering, University of Miyazaki, 1-1 Gakuen Kibanadai Nishi, Miyazaki 889-2192, Japan. *E-mail*: yazaki@cc.miyazaki-u.ac.jp

0 Introduction

Motion by curvature is generally referred as a motion of curves in the plane or surfaces in space which change its shape in time and depend on its bend, especially on its curvature. They are also called curvature flows, since one tracks flows of the family of curves and surfaces parameterized in time. The curvature flow equation is a general term which describes such flows, and has been investigated by many scientists and mathematicians since the 1950's. The crystalline curvature flow equation has been appeared at the end of 1980's by J. E. Taylor, and S. Angenent and M. E. Gurtin.

This lecture will focus mainly on motion of smooth and piecewise linear curves in the plane, and touch on a numerical scheme of crystalline curvature flow equation which is a kind of so-called direct approach. On motion of surfaces, indirect approach (ex. level set methods), other curvature flows, and physical background, the reader is referred to the books by Gurtin [18] and Sethian [32], and the surveys by Taylor, Cahn and Handwerker [38] and Giga [8, 10, 11], and references therein, respectively.

Coming soon! The following two talks will be focused on numerical computation and asymptotic behavior, respectively. In the following first talk,

> **Title:** *On the tangential velocity arising in a crystalline approximation of evolving plane curves,*
> **Workshop:** First Slovak-Japan workshop on Computational Mathematics (Sep., 9-13, 2006) at Bratislava and Kočovce chateu, Slovakia,

I will talk mainly on the following two points:

- Crystalline curvature flow may approximate curvature flow;
- Crystalline algorithm demonstrates how effective it can be as a numerical scheme. In particular, we will see that the tangential velocity plays an important role.

In the following second talk,

> **Title:** *Asymptotic behavior of solutions to an area-preserving motion by crystalline curvature,*
> **Workshop:** Czech-Japanese Seminar in Applied Mathematics 2006 (Sep., 14-16, 2006) at FNSPE CTU in Prague,

I will talk on the asymptotic behavior of the solution polygonal curve of the evolution equation (4.3) in section 4 with some numerical simulations in section 5.

1 Curvature flow equations

To catch mathematical characteristics of curvature flows, we shall formulate the typical problem. Let us consider a curve $\Gamma(t)$ in the plane $\mathbb{R}^2$ parameterized by time t. We mainly focus on embedded and closed curve, and sometimes mention the case where curves are immersed. In any cases, $\Gamma(t)$ is assumed to be orientable.

Note: For example, "∞-like" curve in non-orientable. Although we can calculate evolution of such curve, it is open to interpretation [37].

Plane curves. In the case where $\Gamma(t)$ is a simple, closed and smooth curve, positive direction is assumed to be anticlockwise, i.e., the direction moving on the curve $\Gamma(t)$ with the enclosed region on one's left. By $\boldsymbol{n}$ we denote the unit outward normal vector of $\Gamma(t)$, and by V we denote the growth speed at each point of $\Gamma(t)$ in the direction of $\boldsymbol{n}$. In what follows, we will mainly discuss the normal velocity V depending on the normal vector $\boldsymbol{n}$ and the curvature K in the direction of $-\boldsymbol{n}$. The signed convention of the curvature K is that $K = 1$ if and only if $\Gamma(t)$ is the unit circle. See Figure 1.

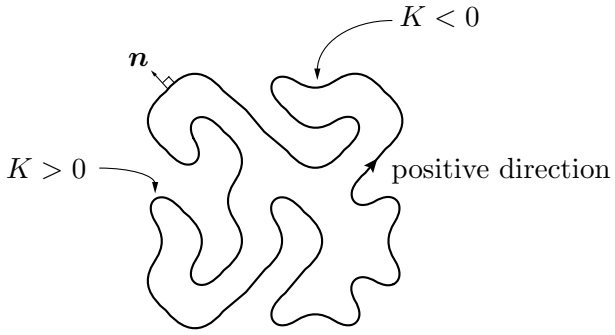

Figure 1: A simple closed curve. In the positive direction, arc-length parameter s is increasing.

Classical curvature flow. The classical and the typical equation which motivates investigation of curvature flow equations is

$$V = -K. \tag{1.1}$$

This is called the **classical curvature flow equation**. Figure 2 indicates evolution of curve by (1.1). Convex part ($K > 0$) of nonconvex curve $\Gamma(t)$ moves towards the direction of $-\boldsymbol{n}$ (inward), and concave part ($K < 0$) moves towards the direction of $\boldsymbol{n}$ (outward). Any embedded curve becomes convex in finite time [17], and any convex curve shrinks to a single point in finite time and its asymptotic shape is a circle [7]. In the case where the solution curve is immersed, for example, the curve has a single small loop as in Figure 3, we can observe that the single loop shrinks and the curve may have cusp in finite time.

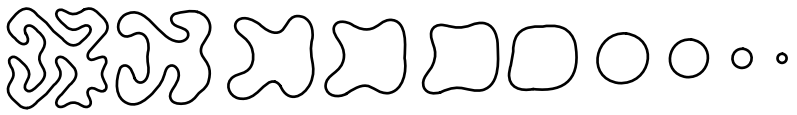

Figure 2: Evolution of a simple closed curve by (1.1) (from left to right).

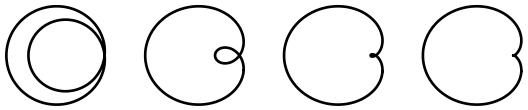

Figure 3: Evolution of a immersed closed curve by (1.1) (from left to right). The small loop disappears in finite time.

A detailed analysis of the singularity near the extinction time was done by Angenent and Velázquez [4].

Example of graph. In the case where $\Gamma(t)$ is described by a graph $y = u(x,t)$, we have the partial differential equation $u_t = \dfrac{u_{xx}}{1+u_x^2}$ equivalent to (1.1) with $V = (0,u_t)^T \cdot \boldsymbol{n}$, $\boldsymbol{n} = \dfrac{(-u_x,1)^T}{\sqrt{1+u_x^2}}$ and $K = \dfrac{-u_{xx}}{(1+u_x^2)^{3/2}}$, where $u_t = \partial u/\partial t$, $u_x = \partial u/\partial x$, $u_{xx} = \partial u_x/\partial x$, and $(a,b)^T = \begin{pmatrix} a \\ b \end{pmatrix}$. Figure 4 indicates its numerical example.

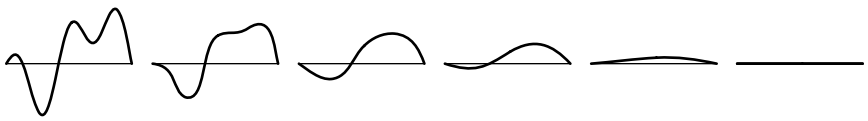

Figure 4: Evolution of a graph $y = u(x,t)$ by the curvature flow equation $u_t = \dfrac{u_{xx}}{1+u_x^2}$ $(0 < x < 1)$ (from left to right). The boundary condition is $u(0) = u(1) = 0$, and the initial curve is given by $u(x,0) = 0.1\sin(\pi x) - 0.3\sin(2\pi x) + 0.2\sin(5\pi x)$.

Gradient flow. As Figure 2 and Figure 4 suggested, the circumference $\mathcal{L}$ of the solution curve $\Gamma(t)$ is decreasing in time. This is the reason why (1.1) is often called the **curve-shortening equation**. Actually, (1.1) is characterized by the gradient flow of $\mathcal{L}$ as follows. Let a simple closed curve is parameterized such as $\Gamma = \left\{\boldsymbol{x}(\theta) \in \mathbb{R}^2;\ \theta \in S^1\right\}$, where $S^1 = \mathbb{R}/2\pi\mathbb{Z}$. As in Figure 1, by s we denote the arc-length parameter. Then the circumference or the total length $\mathcal{L}$ of Γ is given by

$$\mathcal{L}[\Gamma] = \int_\Gamma ds = \int_{S^1} |\boldsymbol{x}_\theta|\, d\theta,$$

since $ds = |\boldsymbol{x}_\theta|\, d\theta$ ($\boldsymbol{x}_\theta = \partial \boldsymbol{x}/\partial\theta$) holds. Now, let ε be a small positive parameter and by $\Gamma_{\varepsilon \boldsymbol{z}}$ we denote small deformation of Γ in the direction of $\boldsymbol{z}$:

$$\Gamma_{\varepsilon \boldsymbol{z}} = \left\{ \boldsymbol{x}(\theta) + \varepsilon \boldsymbol{z}(\theta) \in \mathbb{R}^2;\ \theta \in S^1 \right\}.$$

And we define the rate of variation of $\mathcal{L}[\Gamma]$ in the direction $\boldsymbol{z}$ by

$$\frac{\delta \mathcal{L}[\Gamma]}{\delta \boldsymbol{z}} = \frac{d}{d\varepsilon} \mathcal{L}[\Gamma_{\varepsilon \boldsymbol{z}}]\bigg|_{\varepsilon=0}.$$

Hence the first variation of $\mathcal{L}$ is as follows:

$$\frac{\delta \mathcal{L}[\Gamma]}{\delta \boldsymbol{z}} = \int_\Gamma -\boldsymbol{t}_s \cdot \boldsymbol{z}\, ds, \tag{1.2}$$

where $\boldsymbol{t} = \boldsymbol{n}^\perp$ is the unit tangent vector, $(x_1, x_2)^\perp = (-x_2, x_1)$, $\boldsymbol{t}_s = \partial \boldsymbol{t}/\partial s$, and $\boldsymbol{a} \cdot \boldsymbol{b}$ is the Euclidean inner product between $\boldsymbol{a}$ and $\boldsymbol{b}$. We regard formally the left-hand-side as the inner product $\operatorname{grad} \mathcal{L}[\Gamma] \bullet \boldsymbol{z}$ which is analogue to a directional derivative, and we define this inner product by the right-hand-side. The gradient flow is given by $\boldsymbol{x}_t = -\operatorname{grad} \mathcal{L}[\Gamma] = \boldsymbol{t}_s = -K\boldsymbol{n}$. (Note: The relation $\boldsymbol{n}_s = K\boldsymbol{t}$ and $\boldsymbol{t}_s = -K\boldsymbol{n}$ are known as Frenet-Serret formulae.) Therefore we obtain (1.1): $V = \boldsymbol{x}_t \cdot \boldsymbol{n} = -K$. By means of the above, (1.1) is the equation which requires movement of curve in the most decreasing direction of $\mathcal{L}$ (in the sense of the above inner product).

Exercise 1 Show (1.2).

Remark: The time derivative of $\mathcal{L} = \mathcal{L}(t)$ is given by the following equation:

$$\frac{d}{dt}\mathcal{L}(t) = \frac{\delta \mathcal{L}[\Gamma]}{\delta \boldsymbol{z}}\bigg|_{\boldsymbol{z}=\boldsymbol{x}_t} = \int_\Gamma K\boldsymbol{n} \cdot \boldsymbol{x}_t\, ds = \int_\Gamma KV\, ds.$$

Hence in the case where $V = -K$, we have $\dfrac{d}{dt}\mathcal{L}(t) = -\displaystyle\int_\Gamma K^2\, ds \le 0$, i.e., the curve is shortening in time.

Area-preserving curvature flow. Besides the curve-shortening flow, there has also been interest in area-preserving flows. The typical flow is the gradient flow of $\mathcal{L}$ along curves which enclose a fixed area as follows:

$$V = \overline{K} - K, \tag{1.3}$$

where $\overline{K}$ is the average of K: $\overline{K} = \displaystyle\int_\Gamma K\, ds \Big/ \int_\Gamma ds = 2\pi/\mathcal{L}$ if Γ is simple and closed, $\overline{K} = 2\eta\pi/\mathcal{L}$ if Γ is immersed with the rotation number being $\eta = 2, 3, \ldots$

Exercise 2 The enclosed area $\mathcal{A}$ of Γ is given by

$$\mathcal{A}[\Gamma] = \frac{1}{2}\int_\Gamma \boldsymbol{x}\cdot\boldsymbol{n}\,ds = -\frac{1}{2}\int_{S^1} \boldsymbol{x}\cdot\boldsymbol{x}_\theta^\perp\,d\theta,$$

since the outward normal vector is $\boldsymbol{n} = -\boldsymbol{x}_\theta^\perp/|\boldsymbol{x}_\theta|$. Show the first variation of $\mathcal{A}$:

$$\frac{\delta\mathcal{A}[\Gamma]}{\delta\boldsymbol{z}} = \frac{d}{d\varepsilon}\mathcal{A}[\Gamma_{\varepsilon\boldsymbol{z}}]\bigg|_{\varepsilon=0} = \int_\Gamma \boldsymbol{n}\cdot\boldsymbol{z}\,ds. \tag{1.4}$$

By taking $\boldsymbol{z} = -\operatorname{grad}\mathcal{L}[\Gamma] = \boldsymbol{t}_s$, we have $\displaystyle\int_\Gamma \boldsymbol{n}\cdot\boldsymbol{t}_s\,ds = -\int_\Gamma K\,ds$. Hence by taking $\boldsymbol{z} = \boldsymbol{t}_s - \overline{K}\boldsymbol{n}$, we have $\dfrac{\delta\mathcal{A}[\Gamma]}{\delta\boldsymbol{z}} = 0$. Thus we arrive at equation (1.3).

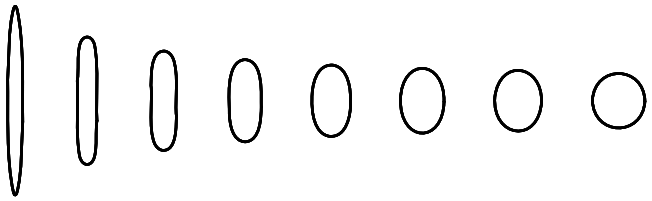

Figure 5: Evolution of a convex curve by (1.3) (from left to right).

Remark: The time derivative of $\mathcal{A} = \mathcal{A}(t)$ is given by the following equation:

$$\frac{d}{dt}\mathcal{A}(t) = \frac{\delta\mathcal{A}[\Gamma]}{\delta\boldsymbol{z}}\bigg|_{\boldsymbol{z}=\boldsymbol{x}_t} = \int_\Gamma \boldsymbol{n}\cdot\boldsymbol{x}_t\,ds = \int_\Gamma V\,ds.$$

Hence in the case where $V = -K$, we have $\dfrac{d}{dt}\mathcal{A}(t) = -\displaystyle\int_\Gamma K\,ds = -2\pi$. Therefore, if Γ is a Jordan curve, then it disappears exactly at the time $2\pi/\mathcal{A}(0)$.

Exercise 3 In the case where $V = \overline{K} - K$, show $\dfrac{d}{dt}\mathcal{L}(t) \le 0$ and $\dfrac{d}{dt}\mathcal{A}(t) = 0$.

Gage [6] proved that any convex curve converges to a circle as time tends to infinity (see Figure 5), and conjectured that a nonconvex curve may intersect; this conjecture was proved rigorously by Mayer and Simonett [30].

Open Problems: The following two problems are still open: One is the problem whether the small loop may shrink or not. Figure 6 is a numerical example, and it suggests that extinction occurs in finite time. The other one is the problem whether any embedded curve becomes eventually convex or not, even if self-intersection occurred. In the curve-shortening case, these problems have been already analyzed, as it was mentioned above.

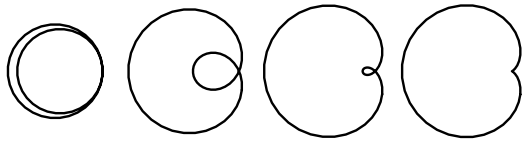

Figure 6: Evolution of a immersed closed curve by (1.3) (from left to right). The small loop disappears in finite time (at least numerically).

2 Basic mathematics I: anisotropy

In the field of material sciences and crystallography, we need to explain the anisotropy — phenomenon of interface motion which depends on the normal direction, i.e., model equations have to contain effects of anisotropy of materials or crystals.

Note: There is two kinds of anisotropy: one is kinetic anisotropy which appears in the problem of growth form, and the other is equilibrium anisotropy which appears in the problem of equilibrium form.

Interfacial energy. For example, if the crystal growth of snow flakes is regarded as motion of closed plane curve, then some points on the interface Γ are easy to growth in the case where their normal directions are in the six special directions. To explain these phenomena, it is convenient to define an interfacial energy on the curve Γ which has line density $\gamma(\boldsymbol{n}) > 0$. Integration of γ over Γ is the total interfacial energy:

$$\mathcal{E}_\gamma[\Gamma] = \int_\Gamma \gamma(\boldsymbol{n})\, ds.$$

In the case where $\gamma \equiv 1$, $\mathcal{E}_\gamma$ is nothing but the total length $\mathcal{L}$, and its gradient flow was (1.1). For a general γ, what is the gradient flow of $\mathcal{E}_\gamma$?

Extension of $\boldsymbol{\gamma}$. The function $\gamma(\boldsymbol{n})$ can be extended to the function $\boldsymbol{x} \in \mathbb{R}^2$ by putting

$$\gamma(\boldsymbol{x}) = \begin{cases} |\boldsymbol{x}|\, \gamma\left(\dfrac{\boldsymbol{x}}{|\boldsymbol{x}|}\right), & \boldsymbol{x} \neq \boldsymbol{0}, \\ 0, & \boldsymbol{x} = \boldsymbol{0}. \end{cases}$$

This extension is called the extension of positively homogeneous of degree 1, since

$$\gamma(\lambda \boldsymbol{x}) = \lambda \gamma(\boldsymbol{x})$$

holds for $\lambda \geq 0$ and $\boldsymbol{x} \in \mathbb{R}^2$. We will use the same notation γ for the extended function. Hereafter we assume that γ is positive for $\boldsymbol{x} \neq \boldsymbol{0}$, and positively homogeneous of degree 1 function.

Remark: The isotropic case $\gamma(\boldsymbol{n}) \equiv 1$ holds if and only if $\gamma(\boldsymbol{x}) = |\boldsymbol{x}|$.

We assume that $\gamma \in C^2(\mathbb{R}^2\backslash\{\boldsymbol{0}\})$. Then the following properties hold:

- $\nabla\gamma(\lambda\boldsymbol{x}) = \nabla\gamma(\boldsymbol{x})$ ($\nabla\gamma$ is homogeneous of degree 0),
- $\gamma(\boldsymbol{x}) = \boldsymbol{x}\cdot\nabla\gamma(\boldsymbol{x})$ (In particular, $\gamma(\boldsymbol{n}) = \boldsymbol{n}\cdot\nabla\gamma(\boldsymbol{n})$ holds),
- $\operatorname{Hess}\gamma(\lambda\boldsymbol{x}) = \dfrac{1}{\lambda}\operatorname{Hess}\gamma(\boldsymbol{x})$ ($\operatorname{Hess}\gamma$ is homogeneous of degree -1),

where $\operatorname{Hess}\gamma = \begin{pmatrix}\gamma_{11} & \gamma_{12}\\ \gamma_{21} & \gamma_{22}\end{pmatrix}$ is the Hessian of γ ($\gamma_{ij} = \partial^2\gamma/\partial x_i\partial x_j$ for $i,j\in\{1,2\}$ and $\boldsymbol{x} = (x_1, x_2)$).

Exercise 4 Show these properties.

Weighted curvature flow. The gradient flow of the total interfacial energy

$$\mathcal{E}_\gamma[\Gamma] = \int_\Gamma \gamma(\boldsymbol{n})\,ds = \int_{S^1}\gamma(-\boldsymbol{x}_\theta^\perp)\,d\theta$$

is $\operatorname{grad}\mathcal{E}_\gamma[\Gamma] = -(\operatorname{Hess}\gamma(\boldsymbol{n})\boldsymbol{t})^\perp K$. Hence the gradient flow is given by $\boldsymbol{x}_t = -\operatorname{grad}\mathcal{E}_\gamma[\Gamma] = (\operatorname{Hess}\gamma(\boldsymbol{n})\boldsymbol{t})^\perp K$, and we obtain the following normal velocity $V = \boldsymbol{x}_t\cdot\boldsymbol{n}$:

$$V = (\operatorname{Hess}\gamma(\boldsymbol{n})\boldsymbol{t})^\perp\cdot\boldsymbol{n}K = -\Lambda_\gamma(\boldsymbol{n}), \tag{2.1}$$

where $\Lambda_\gamma(\boldsymbol{n}) = (\operatorname{Hess}\gamma(\boldsymbol{n})\boldsymbol{n}^\perp)\cdot\boldsymbol{n}^\perp K$. This $\Lambda_\gamma(\boldsymbol{n})$ is called **weighted curvature** or **anisotropic curvature**, and (2.1) is called the **weighted curvature flow equation** or **anisotropic curvature flow equation**.

Exercise 5 Show $\operatorname{grad}\mathcal{E}_\gamma[\Gamma] = -(\operatorname{Hess}\gamma(\boldsymbol{n})\boldsymbol{t})^\perp K$.

Exercise 6 Try the calculation of the gradient flow of $\mathcal{E}_\gamma[\Gamma] = \displaystyle\int_\Gamma \gamma(\boldsymbol{x})\,ds$, i.e., this is the case where the line density γ depends on the position $\boldsymbol{x}$.

Weighted curvature. Meaning of the weighted curvature $\Lambda_\gamma(\boldsymbol{n})$ will be more clearly as follows: Let θ be the exterior normal angle such as $\boldsymbol{n} = \boldsymbol{n}(\theta) = (\cos\theta, \sin\theta)$ and $\boldsymbol{t} = \boldsymbol{t}(\theta) = (-\sin\theta, \cos\theta)$. Put $\widehat{\gamma}(\theta) = \gamma(\boldsymbol{n}(\theta))$ defined on S^1. Then we obtain

$$\Lambda_\gamma(\boldsymbol{n}(\theta)) = (\widehat{\gamma}(\theta) + \widehat{\gamma}''(\theta))K,$$

where $\widehat{\gamma}''(\theta) = d\widehat{\gamma}'(\theta)/d\theta$, $\widehat{\gamma}'(\theta) = d\widehat{\gamma}(\theta)/d\theta$.

Exercise 7 Show this equation.

Example of $\boldsymbol{\gamma}$. Let us construct an example of characteristic γ. For a natural number M, we extend the line segment $y = x$ ($x \in [0, 2\pi/M]$) to $2\pi/M$-periodic function $p(x)$ such as

$$p(x) = \frac{2}{M}\left(\arctan\left(\tan\left(\frac{M}{2}x - \frac{\pi}{2}\right)\right) + \frac{\pi}{2}\right),$$

and by $g(x)$ we denote a concave and symmetric function with respect to the central line $x = \pi/M$ defined on $[0, 2\pi/M]$. For example,

$$g(x) = \frac{\sin x + \sin(2\pi/M - x)}{\sin(2\pi/M)}.$$

The following function γ_p is a $2\pi/M$-periodic function with the number of peak being M on $[0, 2\pi/M]$ (Figure 8 (left)).

$$\gamma_p(\theta) = g(p(\theta)), \quad \theta \in \mathbb{R}.$$

Note that γ_p is not differentiable at $2\pi k/M$ ($k \in \mathbb{Z}$). Then by using $\rho_\mu(x) = \sqrt{x^2 + \mu^{-2}}$, we construct a smooth function γ_μ (Figure 8 (left)):

$$\gamma_\mu(\theta) = \rho_\mu(\gamma_p(\theta) - 1) + 1, \quad \theta \in \mathbb{R}.$$

As μ tends to infinity, $\rho_\mu(x)$ converges to $|x|$, and then γ_μ converges to γ_p formally.

In general, if the curve $\Gamma(t)$ is strictly convex, then the solution K of (2.1) satisfies the partial differential equation $K_t = K^2((-V)_{\theta\theta} + (-V))$ ($V_{\theta\theta} = \partial^2 V/\partial\theta^2$). See the book of Gurtin [18] or Exercise 8 below. Hence if $\widehat{\gamma} + \widehat{\gamma}'' > 0$ holds, then the PDE is quasi-linear strictly parabolic type and its Cauchy problem is solvable. We note that γ_μ satisfies $\gamma_\mu + \gamma_\mu'' > 0$.

Exercise 8 Check the following story: Using the hight function $h = \boldsymbol{x} \cdot \boldsymbol{n}$, the curve $\Gamma = \{\boldsymbol{x}\}$ is described as $\boldsymbol{x} = h\boldsymbol{n} + h_\theta \boldsymbol{t}$, if Γ is strictly convex. Hence $h_{\theta\theta} = K^{-1} - h$ holds, and then we have $(K^{-1})_t = V_{\theta\theta} + V$ by $V = h_t$.

Figure 7 indicates evolution of solution curves of (2.1) by using the interfacial energy density $\widehat{\gamma} = \gamma_\mu$ in the case where $M = 6$ and $\mu = 15$. The asymptotic shape seems to be a round hexagon which is strikingly different from the one in Figure 2.

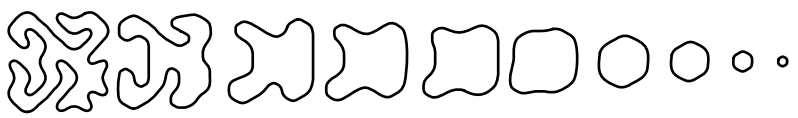

Figure 7: Evolution of a simple closed curve by (2.1) (from left to right). The initial curve is the same as in Figure 2.

3 Basic mathematics II: the Wulff shape, etc.

We will consider γ_p and γ_μ by graphical constructions.

The Frank diagram. Figure 8 (left) indicates the graph of $\gamma = \gamma_p(\theta)$ and $\gamma = \gamma_p(\theta)$, respectively; and Figure 8 (middle) indicates the polar coordinate of each γ:

$$\mathcal{C}_\gamma = \left\{ \gamma(\boldsymbol{n}(\theta))\boldsymbol{n}(\theta);\ \theta \in S^1 \right\}.$$

Incidentally, to observe the characteristic of γ, the following **Frank diagram** (Figure 8 (right)) is more useful than a graph of γ and $\mathcal{C}_\gamma$:

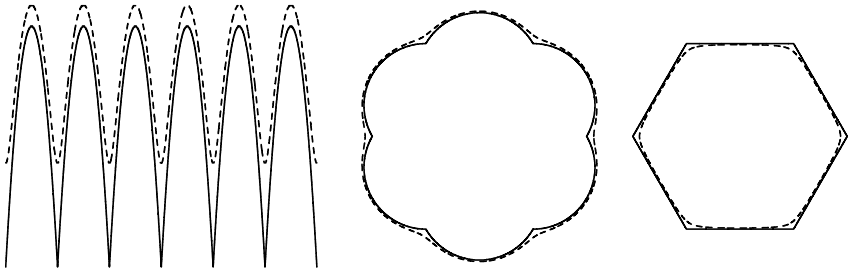

Figure 8: In each figure, the solid line is $\gamma_p(\theta)$, and the dotted line is $\gamma_\mu(\theta)$ ($\mu = 15$), respectively. $M = 6$ in any case. (Left): graphs of $\gamma_p(\theta)$ and $\gamma_\mu(\theta)$. The horizontal axis is $0 \le \theta \le 2\pi$, and the vertical axis is magnified for easy to observe. At each point $\theta = 2\pi k/M$ ($k \in \mathbb{Z}$), the function $\gamma_p(\theta)$ (resp. $\gamma_\mu(\theta)$) achieves the minimum value 1 (resp. $1+1/\mu$). (Middle): $\mathcal{C}_{\gamma_p}$ and $\mathcal{C}_{\gamma_\mu}$. (Right): the Frank diagram $\mathcal{F}_{\gamma_p}$ and $\mathcal{F}_{\gamma_\mu}$. $\mathcal{F}_{\gamma_p}$ is a regular M-polygon.

$$\mathcal{F}_\gamma = \left\{ \frac{\boldsymbol{n}(\theta)}{\gamma(\boldsymbol{n}(\theta))};\ \theta \in S^1 \right\} = \left\{ \boldsymbol{x} \in \mathbb{R}^2;\ \gamma(\boldsymbol{x}) = 1 \right\}.$$

From this definition $\mathcal{F}_\gamma = \mathcal{C}_{1/\gamma}$ holds.

Exercise 9 Show the following three proposition are equivalent.

(1) The set enclosed by $\mathcal{F}_\gamma$, say $F = \left\{ \boldsymbol{x} \in \mathbb{R}^2;\ \gamma(\boldsymbol{x}) \le 1 \right\}$, is convex.

(2) The function γ satisfies $\gamma((1-\lambda)\boldsymbol{x} + \lambda\boldsymbol{y}) \le (1-\lambda)\gamma(\boldsymbol{x}) + \lambda\gamma(\boldsymbol{y})$ for $\boldsymbol{x}, \boldsymbol{y} \in \mathbb{R}^2$ and $\lambda \in [0,1]$. (That is, γ is convex.)

(3) The function γ satisfies $\gamma(\boldsymbol{x} + \boldsymbol{y}) \le \gamma(\boldsymbol{x}) + \gamma(\boldsymbol{y})$ for $\boldsymbol{x}, \boldsymbol{y} \in \mathbb{R}^2$. (That is, γ is subadditive.)

The interfacial energy γ can be classified by the Frank diagram $\mathcal{F}_\gamma$. Since the sign of the curvature of the curve $\mathcal{F}_\gamma$ agrees with the sign of $\widehat{\gamma} + \widehat{\gamma}''$, then as mentioned above, the initial value problem of (2.1) can be caught in the framework of parabolic partial

differential equations. The function $\gamma = \gamma_\mu$ is such an example. However, in the case where $\gamma = \gamma_p$, its Frank diagram $\mathcal{F}_{\gamma_p}$ is a regular M-polygon, and on the each edge $\widehat{\gamma}_p + \widehat{\gamma}_p'' = 0$, and $\widehat{\gamma}_p$ may not be differentiable at each vertex. To treat such interfacial energy, crystalline curvature flow in the title will enter the stage. It will be mentioned later. Before it, let us define another shape of characterizing γ.

The Wulff shape. The following shape is called the **Wulff shape**:

$$\mathcal{W}_\gamma = \bigcap_{\theta \in S^1} \left\{ \boldsymbol{x} \in \mathbb{R}^2;\ \boldsymbol{x} \cdot \boldsymbol{n}(\theta) \le \gamma(\boldsymbol{n}(\theta)) \right\}.$$

Figure 9 indicates the Wulff shape of γ_p and γ_μ, respectively, in the case where $M = 4$ and $M = 6$.

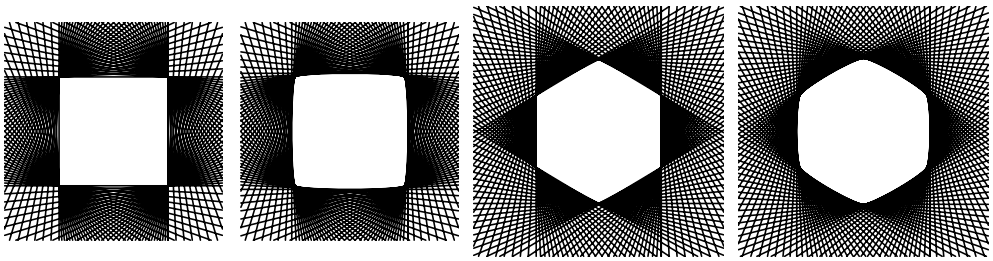

Figure 9: Comparison of $\gamma_p(\theta)$ and $\gamma_\mu(\theta)$ ($\mu = 15$) by the Wulff shape. (Left, middle left): The Wulff shapes $\mathcal{W}_{\gamma_p}$ and $\mathcal{W}_{\gamma_\mu}$ with $M = 4$. (Middle right, right): The Wulff shapes $\mathcal{W}_{\gamma_p}$ and $\mathcal{W}_{\gamma_\mu}$ with $M = 6$. Two $\mathcal{W}_{\gamma_p}$'s are regular M-polygons, and two $\mathcal{W}_{\gamma_\mu}$'s are round regular M-polygons, respectively.

The Wulff shape is a convex set by means of constructions. In particular, if γ is smooth and $\mathcal{F}_\gamma$ is strictly convex, then $\mathcal{W}_\gamma$ is also a strictly convex set with a smooth boundary. In this case, the distance from the origin (which is inside of $\mathcal{W}_\gamma$) to L_θ equals to $\gamma(\boldsymbol{n}(\theta)) = \widehat{\gamma}(\theta)$, where L_θ is the tangent line which is passing through the point on $\partial\mathcal{W}_\gamma$ with its outward normal vector being $\boldsymbol{n}(\theta)$. From this fact, we note that the curvature of $\partial\mathcal{W}_\gamma$ is given by $(\widehat{\gamma} + \widehat{\gamma}'')^{-1}$.

Exercise 10 Show that the curvature of $\partial\mathcal{W}_\gamma$ is $(\widehat{\gamma} + \widehat{\gamma}'')^{-1}$ if $\mathcal{W}_\gamma$ is a strictly convex set with a smooth boundary.

In the physical context, $\mathcal{W}_\gamma$ describes the equilibrium of crystal, i.e., in the plane case, $\mathcal{W}_\gamma$ is the answer of the following ≪Wulff problem≫ on the equilibrium shape of crystals (by Gibbs (1878), Curie (1885), and Wulff (1901)):

> What is the shape which has the least total interfacial energy $\mathcal{E}_\gamma$ of the curve for the fixed enclosed area? That is, "$\underset{\Gamma}{\text{Minimize}}\, \mathcal{E}_\gamma[\Gamma]$ subject to $\mathcal{A}[\Gamma] \equiv const.$"

This suggests that the asymptotic shape of a solution curve of the gradient flow of $\mathcal{E}_\gamma$ (2.1) is $\partial\mathcal{W}_{\gamma_\mu}$ in the case $\gamma = \gamma_\mu$ (Figure 7). However, in the mathematical context, known results are not so much.

Open Problems: Convexified phenomena or formation of convexity is one of the interesting problems. In the isotropic case $\widehat{\gamma} \equiv 1$, Grayson [17] proved that convexity is formed (see Figure 2). However in the anisotropic case, even if γ is smooth, the formation of convexity has not been completed, except in the symmetric case $\widehat{\gamma}(\theta + \pi) = \widehat{\gamma}(\theta)$ by Chou and Zhu [5].

Incidentally, the Frank diagram $\mathcal{F}_\gamma$ has been considered after the Wulff shape $\mathcal{W}_\gamma$ has appeared (Frank (1963) and Meijering (1963)). See the book on crystal growth in detail. We also refer the reader to Kobayashi and Giga [29] for a lot of examples of $\mathcal{C}_\gamma$, $\mathcal{F}_\gamma$ and $\mathcal{W}_\gamma$, and for discussion of anisotropy and the effect of curvature.

Numerical examples. Now, going back the story, we observe the behavior of a solution curve $y = u(x,t)$ by (2.1) with $\gamma = \gamma_\mu$ ($\mu = 1000$) from a view point of an approximation of $\gamma = \gamma_p$.

Since the total interfacial energy is given by

$$\mathcal{E}_\gamma = \int_0^1 W(u_x)\,dx, \quad W(u_x) = \widehat{\gamma}(\theta)\sqrt{1+u_x^2}, \quad \theta = -\arctan\frac{1}{u_x},$$

we obtain the partial differential equation

$$u_t = \sqrt{1+u_x^2}\,(W'(u_x))_x = \frac{\widehat{\gamma}+\widehat{\gamma}''}{1+u_x^2}u_{xx},$$

which is equivalent to (2.1).

Figure 10 indicates a numerical example of the case where $M = 4$ and $\mu = 1000$. As time goes by, one can observe that line segment parts satisfying $u_x = 0$ expands, and the other parts (which are put between two parallel line segments satisfying $u_x = 0$) do not move, and will disappear in finite time. Actually, since $\widehat{\gamma}_\mu + \widehat{\gamma}_\mu''$ takes a huge value only at $\theta = \dfrac{\pi}{2}k$ ($k \in \mathbb{Z}$) and almost zero at other points, the movement of points satisfying $u_x \sim 0$ can be observed and other points do not seem to move.

Figure 11 indicates a numerical example of the case where $M = 6$ and $\mu = 1000$. In this case, $\mathcal{W}_\gamma$ is almost a regular hexagon (it almost agrees with $\mathcal{W}_{\gamma_p}$ in Figure 9 (middle right), and in the set of normal angles of $\mathcal{W}_{\gamma_\mu}$ one can observe the movement of points on the graph satisfying that their normal angles almost agree with $\theta = \pm\dfrac{\pi}{3}k$ ($k = 1, 2$), and other points do not seem to move. Since the end points are fixed, Figure 11 (far right) is the final shape.

When μ tends to infinity, how does the equation $u_t = \sqrt{1+u_x^2}\,(W'(u_x))_x$ change? In the case where $M = 4$, $\widehat{\gamma}_p(\theta) = |\cos\theta| + |\sin\theta|$ holds, and then we have $W(u_x) = |u_x| + 1$. From this we obtain formally $W''(u_x) = 2\delta(u_x)$, i.e., the partial differential equation

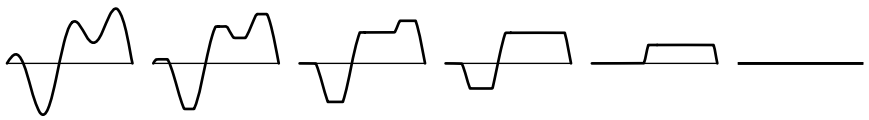

Figure 10: Evolution of a graph $y = u(x,t)$ by the curvature flow equation $u_t = \sqrt{1+u_x^2}\,(W'(u_x))_x$ $(0 < x < 1)$ (from left to right). Here $W(u_x) = \widehat{\gamma}_\mu(\theta)\sqrt{1+u_x^2}$ $(\mu = 1000, M = 4)$, $\theta = \dfrac{\pi}{2} + \arctan u_x$. The boundary conditions are $u(0) = u(1) = 0$, and the initial curve is the same as the one in Figure 4.

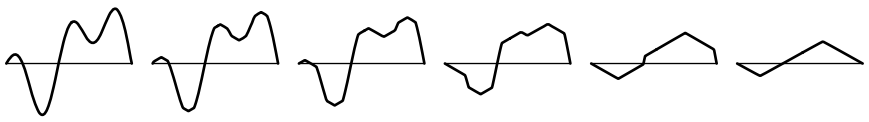

Figure 11: Evolution of a graph $y = u(x,t)$ by the curvature flow equation $u_t = \sqrt{1+u_x^2}\,(W'(u_x))_x$ $(0 < x < 1)$ (from left to right). Here $W(u_x) = f_\mu(\theta)\sqrt{1+u_x^2}$ $(\mu = 1000, M = 6)$, $\theta = \dfrac{\pi}{2} + \arctan u_x$. The boundary conditions are $u(0) = u(1) = 0$, and the initial curve is the same as the one in Figure 4.

becomes $u_t = 2\sqrt{1+u_x^2}\delta(u_x)u_{xx}$, where δ is Dirac delta function. As Figure 10 suggested, the right-hand-side is considerable as a nonlocal quantity [9].

By the observation of Figure 10 and Figure 11, it seems that there is no problem if curves are restricted to the following special class of polygonal curves: the set of normal vectors of the curves agrees with the one of the Wulff shape.

4 Crystalline curvature flow equation

We will define crystalline curvature flow equations.

Polygonal curves. Let $\mathcal{P}$ be a simple closed N-sided polygonal curve in the plane $\mathbb{R}^2$, and label the position vector of vertices $\boldsymbol{p}_i$ $(i = 1, 2, \ldots, N)$ in an anticlockwise order:

$$\mathcal{P} = \bigcup_{i=1}^{N} \mathcal{S}_i,$$

where $\mathcal{S}_i = [\boldsymbol{p}_i, \boldsymbol{p}_{i+1}]$ is the i-th edge $(\boldsymbol{p}_{N+1} = \boldsymbol{p}_1)$. The length of $\mathcal{S}_i$ is $d_i = |\boldsymbol{p}_{i+1} - \boldsymbol{p}_i|$, and then the i-th unit tangent vector is $\boldsymbol{t}_i = (\boldsymbol{p}_{i+1} - \boldsymbol{p}_i)/d_i$ and the i-th unit outward normal vector is $\boldsymbol{n}_i = -\boldsymbol{t}_i^{\perp}$, where $(a,b)^{\perp} = (-b,a)$. Put $\mathcal{N} = \{\boldsymbol{n}_1, \boldsymbol{n}_2, \ldots, \boldsymbol{n}_N\}$. Let θ_i be the exterior normal angle of $\mathcal{S}_i$. Then $\boldsymbol{n}_i = \boldsymbol{n}(\theta_i)$ and $\boldsymbol{t}_i = \boldsymbol{t}(\theta_i)$ hold. We define the i-th hight function $h_i = \boldsymbol{p}_i \cdot \boldsymbol{n}_i = \boldsymbol{p}_{i+1} \cdot \boldsymbol{n}_i$. See Figure 12. By using N-tuple $h = (h_1, h_2, \ldots, h_N)$, d_i is described as follows:

$$d_i[h] = \frac{\chi_{i-1,i}}{\sqrt{1-(\boldsymbol{n}_{i-1}\cdot\boldsymbol{n}_i)^2}}(h_{i-1} - (\boldsymbol{n}_{i-1}\cdot\boldsymbol{n}_i)h_i) + \frac{\chi_{i,i+1}}{\sqrt{1-(\boldsymbol{n}_i\cdot\boldsymbol{n}_{i+1})^2}}(h_{i+1} - (\boldsymbol{n}_i\cdot\boldsymbol{n}_{i+1})h_i),$$

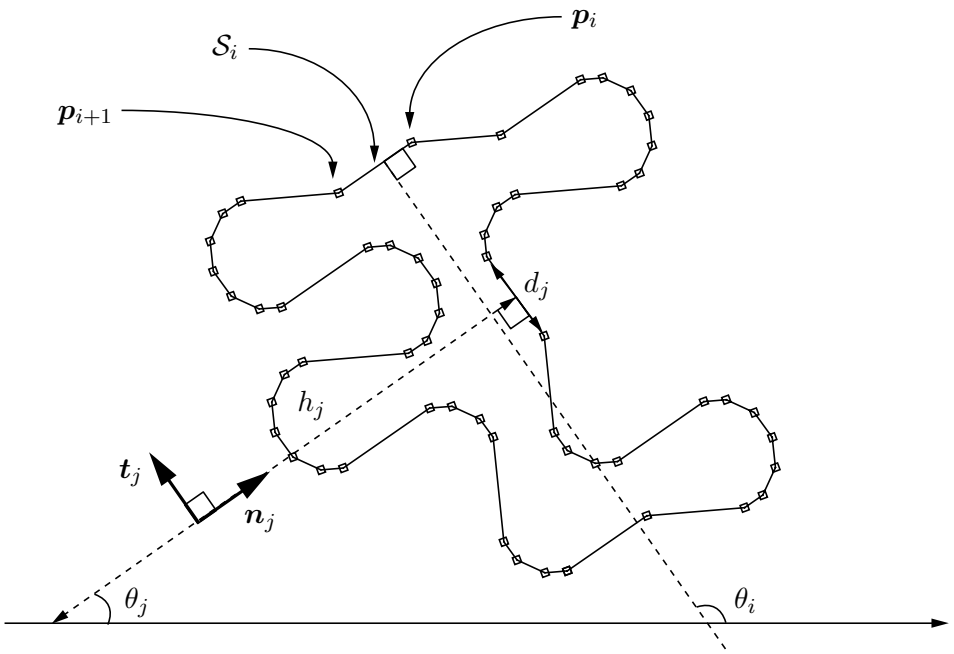

Figure 12: Example of polygonal curves ($N = 56$).

where $\chi_{i,j} = \mathrm{sgn}(\det(\boldsymbol{n}_i, \boldsymbol{n}_j))$ for $i = 1, 2, \ldots, N$ ($h_{N+1} = h_1, h_0 = h_N$). Since $\boldsymbol{n}_i \cdot \boldsymbol{n}_j = \cos(\theta_i - \theta_j)$, we have another expression:

$$d_i[h] = -(\cot\vartheta_i + \cot\vartheta_{i+1})h_i + h_{i-1}\,\mathrm{cosec}\,\vartheta_i + h_{i+1}\,\mathrm{cosec}\,\vartheta_{i+1}, \tag{4.1}$$

where $\vartheta_i = \theta_i - \theta_{i-1}$ for $i = 1, 2, \ldots, N$. Note that $0 < |\vartheta_i| < \pi$ holds for all i. Furthermore, the i-th vertex $\boldsymbol{p}_i$ ($i = 1, 2, \ldots, N$) is described as follows:

$$\boldsymbol{p}_i = h_i\boldsymbol{n}_i + \frac{h_{i-1} - (\boldsymbol{n}_{i-1} \cdot \boldsymbol{n}_i)h_i}{\boldsymbol{n}_{i-1} \cdot \boldsymbol{t}_i}\boldsymbol{t}_i. \tag{4.2}$$

Exercise 11 Check that $d_i = |\boldsymbol{p}_{i+1} - \boldsymbol{p}_i|$ and $d_i = (\boldsymbol{p}_{i+1} - \boldsymbol{p}_i) \cdot \boldsymbol{t}_i$ hold.

Exercise 12 Fix any $\boldsymbol{a} \in \mathbb{R}^2$. By $s_i = \boldsymbol{a} \cdot \boldsymbol{n}_i$ we denote distance from the origin to $\boldsymbol{a}$ in the direction $\boldsymbol{n}$, and by $s = (s_1, s_2, \ldots, s_N)$ we denote their N-tuple ($s_{N+1} = s_1, s_0 = s_N$). Show that $d_i[s] = 0$ holds for all $i = 1, 2, \ldots, N$. From this fact, $d_i[h + s] = d_i[h] + d_i[s] = d_i[h]$ holds for all i. This means that the shape of curve does not change for a shift of the origin.

Crystalline energy. If the Frank diagram $\mathcal{F}_\gamma$ is a convex polygon, γ is called **crystalline energy**. When $\mathcal{F}_\gamma$ is a J-sided convex polygon, there exists a set of angles $\{\phi_i \,|\, \phi_1 < \phi_2 < \cdots < \phi_J < \phi_1 + 2\pi\}$ such that the position vectors of vertices are labeled $\boldsymbol{n}(\phi_i)/\gamma(\boldsymbol{n}(\phi_i))$ in an anticlockwise order ($\phi_{J+1} = \phi_1$):

$$\mathcal{F}_\gamma = \bigcup_{i=1}^{J} \left[\frac{\boldsymbol{\nu}_i}{\gamma(\boldsymbol{\nu}_i)}, \frac{\boldsymbol{\nu}_{i+1}}{\gamma(\boldsymbol{\nu}_{i+1})} \right].$$

Here and hereafter, we denote $\boldsymbol{\nu}_i = \boldsymbol{n}(\phi_i)$ $(\forall i)$. See Figure 13 (left). In this case, the Wulff shape is also a J-sided convex polygon with the outward normal vector of the i-th edge being $\boldsymbol{\nu}_i$:

$$\mathcal{W}_\gamma = \bigcap_{i=1}^{J} \left\{ \boldsymbol{x} \in \mathbb{R}^2;\ \boldsymbol{x} \cdot \boldsymbol{\nu}_i \le \gamma(\boldsymbol{\nu}_i) \right\}.$$

See Figure 13 (right). Put $\mathcal{N}_\gamma = \{\boldsymbol{\nu}_1, \boldsymbol{\nu}_2, \ldots, \boldsymbol{\nu}_J\}$.

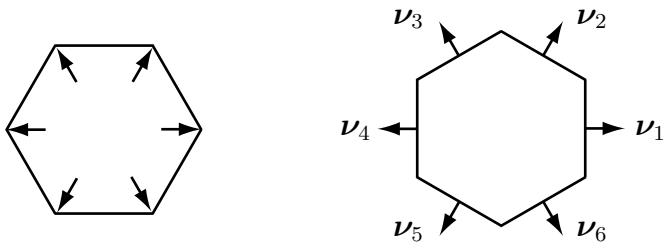

Figure 13: Examples of the Frank diagram (left) and the Wulff shape (right) in the case where γ is a crystalline energy and $J = 6$. This Frank diagram is the same regular hexagon $\mathcal{F}_{\gamma_p}$ as in Figure 8 (right), and this Wulff shape is the same regular hexagon $\mathcal{W}_{\gamma_p}$ as in Figure 9 (middle right).

Remark: Fix any $i = 1, 2, \ldots, J$. The point on the i-th edge of Frank polygon $\mathcal{F}_\gamma$ is

$$\frac{\boldsymbol{\nu}}{\gamma(\boldsymbol{\nu})} = (1-\mu)\frac{\boldsymbol{\nu}_{i-1}}{\gamma(\boldsymbol{\nu}_{i-1})} + \mu\frac{\boldsymbol{\nu}_i}{\gamma(\boldsymbol{\nu}_i)}$$

for some $\mu \in (0,1)$, where $\boldsymbol{\nu}$ is the unit vector in the direction between $\boldsymbol{\nu}_{i-1}$ and $\boldsymbol{\nu}_i$:

$$\boldsymbol{\nu} = \frac{(1-\lambda)\boldsymbol{\nu}_{i-1} + \lambda\boldsymbol{\nu}_i}{|(1-\lambda)\boldsymbol{\nu}_{i-1} + \lambda\boldsymbol{\nu}_i|}, \quad \lambda = \frac{\mu\gamma(\boldsymbol{\nu}_{i-1})}{(1-\mu)\gamma(\boldsymbol{\nu}_i) + \mu\gamma(\boldsymbol{\nu}_{i-1})}.$$

Note that $\gamma((1-\mu)\boldsymbol{\nu}_i + \mu\boldsymbol{\nu}_{i-1}) = (1-\mu)\gamma(\boldsymbol{\nu}_i) + \mu\gamma(\boldsymbol{\nu}_{i-1})$ holds. By $\boldsymbol{y}$, we denote the i-th vertex of the Wulff polygon $\mathcal{W}_\gamma$:

$$\boldsymbol{y} = \gamma(\boldsymbol{\nu}_i)\boldsymbol{\nu}_i + \frac{\gamma(\boldsymbol{\nu}_{i-1}) - (\boldsymbol{\nu}_{i-1}\cdot\boldsymbol{\nu}_i)\gamma(\boldsymbol{\nu}_i)}{\boldsymbol{\nu}_{i-1}\cdot\boldsymbol{\nu}_i^\perp}\boldsymbol{\nu}_i^\perp.$$

Then the following equation holds:

$$\boldsymbol{y}\cdot\boldsymbol{\nu} = \gamma(\boldsymbol{\nu}).$$

Exercise 13 Check $\boldsymbol{y}\cdot\boldsymbol{\nu} = \gamma(\boldsymbol{\nu})$.

Admissible curves. Following [22], we call $\mathcal{P}$ an **essentially admissible** curve if and only if the outward unit normal vectors $\boldsymbol{n}_i, \boldsymbol{n}_{i+1} \in \mathcal{N}$ $(\boldsymbol{n}_{N+1} = \boldsymbol{n}_1)$ satisfy

$$\boldsymbol{n}_{i+\lambda} = \frac{(1-\lambda)\boldsymbol{n}_i + \lambda\boldsymbol{n}_{i+1}}{|(1-\lambda)\boldsymbol{n}_i + \lambda\boldsymbol{n}_{i+1}|} \notin \mathcal{N}_\gamma$$

for $\lambda \in (0,1)$ and $i = 1, 2, \ldots, N$. See Figure 14 (middle).

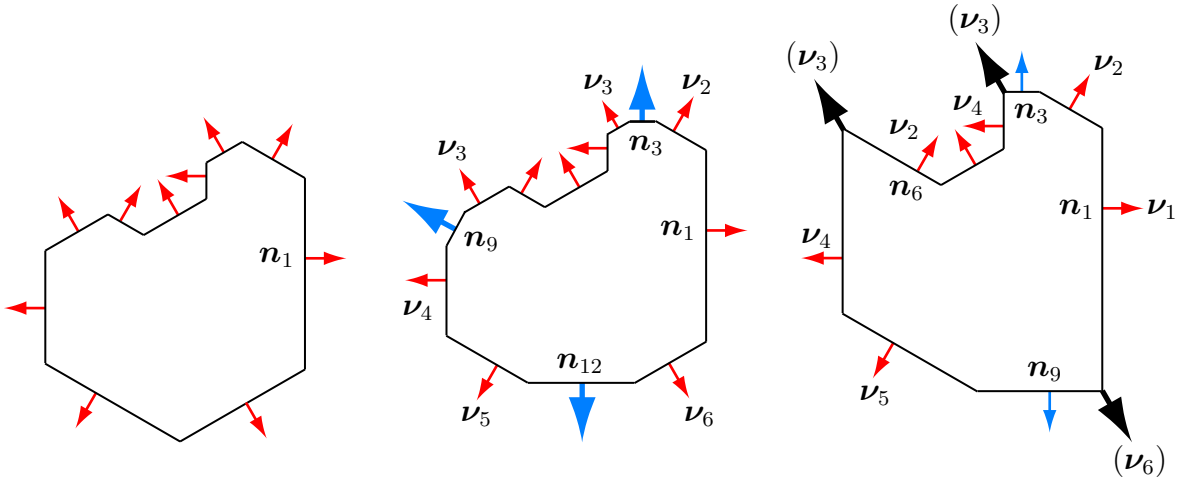

Figure 14: Three typical examples of polygonal curves for the Wulff shape in Figure 13 (right). (Left): admissible polygonal curve ($N = 10$). (Middle): essentially admissible polygonal curve ($N = 13$). Note that $\mathcal{N}_\gamma \oplus \{\boldsymbol{n}_3, \boldsymbol{n}_9, \boldsymbol{n}_{12}\} = \mathcal{N}$ holds. (Right): this polygonal curve ($N = 9$) is not admissible, nor essentially admissible, since $\mathcal{N}_\gamma \not\supseteq \mathcal{N}$ ($\boldsymbol{\nu}_6 \notin \mathcal{N}$) holds, and in addition there exist $\lambda, \lambda', \lambda'' \in (0,1)$ such that $\boldsymbol{n}_{3+\lambda} = \boldsymbol{n}_{6+\lambda'} = \boldsymbol{\nu}_3, \boldsymbol{n}_{9+\lambda''} = \boldsymbol{\nu}_6 \in \mathcal{N}_\gamma$ holds.

Exercise 14 If $\mathcal{P}$ is an essentially admissible curve, then $\mathcal{N} \supseteq \mathcal{N}_\gamma$ holds. But the reverse is not true. Make a counterexample.

Remark: In the case where $\mathcal{P}$ is a convex polygon, $\mathcal{P}$ is an essentially admissible if and only if $\mathcal{N} \supseteq \mathcal{N}_\gamma$ holds.

Exercise 15 Check this remark.

We call $\mathcal{P}$ an **admissible** curve if and only if $\mathcal{P}$ is an essentially admissible curve and $\mathcal{N} = \mathcal{N}_\gamma$ (especially, $\mathcal{N} \subseteq \mathcal{N}_\gamma$) holds. In other words, $\mathcal{P}$ is admissible if and only if $\mathcal{N} = \mathcal{N}_\gamma$ holds and any adjacent two normal vectors in the set $\mathcal{N}_\gamma$, for example $\boldsymbol{\nu}_i$ and $\boldsymbol{\nu}_{i+1}$ are also adjacent in the set $\mathcal{N}$, i.e., $\{\boldsymbol{\nu}_i, \boldsymbol{\nu}_{i+1}\} = \{\boldsymbol{n}_j, \boldsymbol{n}_{j+1}\} \subset \mathcal{N}$ holds for some i and j ($\boldsymbol{\nu}_{J+1} = \boldsymbol{\nu}_1$, $\boldsymbol{n}_{N+1} = \boldsymbol{n}_1$). See Figure 14 (left).

Gradient of the total energy. Let $\mathcal{P}$ be an essentially admissible N-sided curve with the N-tuple of hight functions $h = (h_1, h_2, \ldots, h_N)$. Then the total interfacial (crystalline) energy on $\mathcal{P}$ is

$$\mathcal{E}_\gamma[h] = \sum_{i=1}^{N} \gamma(\boldsymbol{n}_i) d_i[h].$$

For two N-tuples $\varphi = (\varphi_1, \varphi_2, \ldots, \varphi_N), \psi = (\psi_1, \psi_2, \ldots, \psi_N) \in \mathbb{R}^N$, let us define the inner product on $\mathcal{P}$ as follows:

$$(\varphi, \psi)_2 = \sum_{i=1}^{N} \varphi_i \psi_i d_i[h].$$

Furthermore, we define the rate of variation of $\mathcal{E}_\gamma[h]$ in the direction φ and the first variation $\dfrac{\delta\mathcal{E}_\gamma[h]}{\delta h}$ as follows:

$$\frac{\delta\mathcal{E}_\gamma[h]}{\delta\varphi} = \frac{d}{d\varepsilon}\mathcal{E}_\gamma[h+\varphi]\bigg|_{\varepsilon=0} = \operatorname{grad}\mathcal{E}_\gamma[h]\bullet\varphi = \left(\frac{\delta\mathcal{E}_\gamma[h]}{\delta h},\varphi\right)_2.$$

Crystalline curvature. The first variation of $\mathcal{E}_\gamma[h]$ of $\mathcal{P}$ at $\mathcal{S}_i$ is

$$\frac{\delta\mathcal{E}_\gamma[h]}{\delta\varphi} = \sum_{i=1}^{N}\gamma(\boldsymbol{n}_i)d_i[\varphi] = \sum_{i=1}^{N}d_i[\gamma]\varphi_i = \sum_{i=1}^{N}\frac{d_i[\gamma]}{d_i[h]}\varphi_i d_i[h],$$

where $\gamma=(\gamma(\boldsymbol{n}_1),\gamma(\boldsymbol{n}_2),\dots,\gamma(\boldsymbol{n}_N))$. Hence we have $\left(\dfrac{\delta\mathcal{E}_\gamma[h]}{\delta h}\right)_i = \dfrac{d_i[\gamma]}{d_i[h]}$ for $i=1,2,\dots,N$ in this metric $(\cdot,\cdot)_2$. This is called **crystalline curvature** on the i-th edge $\mathcal{S}_i$, and we denote it by $\Lambda_\gamma(\boldsymbol{n}_i)$:

$$\Lambda_\gamma(\boldsymbol{n}_i) = \left(\frac{\delta\mathcal{E}_\gamma[h]}{\delta h}\right)_i = \frac{d_i[\gamma]}{d_i[h]}, \quad i=1,2,\dots,N.$$

The numerator is described as

$$d_i[\gamma] = \chi_i l_\gamma(\boldsymbol{n}_i),$$

where $\chi_i=(\chi_{i-1,i}+\chi_{i,i+1})/2$ takes $+1$ (resp. -1) if $\mathcal{P}$ is convex (resp. concave) around $\mathcal{S}_i$ in the direction of $-\boldsymbol{n}_i$, otherwise $\chi_i=0$; and $l_\gamma(\boldsymbol{n})$ is the length of the j-th edge of $\mathcal{W}_\gamma$ if $\boldsymbol{n}=\boldsymbol{\nu}_j$ for some j, otherwise $l_\gamma(\boldsymbol{n})=0$.

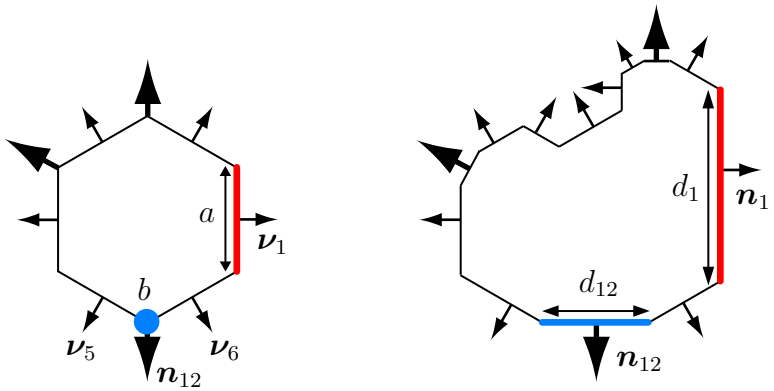

Figure 15: The Wulff shape (left) is the same hexagon as in Figure 13 (right). Essentially admissible polygonal curve (right) is the same curve as in Figure 14 (middle). (Left): a is the length of edge $l_\gamma(\boldsymbol{n}_1)>0$ and b is the length of degenerate edge $l_\gamma(\boldsymbol{n}_{12})=0$. (Right): d_1 (resp. d_{12}) is the length of the edge whose normal vector is $\boldsymbol{n}_1$ (resp. $\boldsymbol{n}_{12}$). Hence the crystalline curvature is $\Lambda(\boldsymbol{n}_1)=l_\gamma(\boldsymbol{n}_1)/d_1$ (resp. $\Lambda(\boldsymbol{n}_{12})=0$).

Remark: If $\mathcal{P}$ is an admissible and convex polygon, then $\boldsymbol{n}_i = \boldsymbol{\nu}_i$ and $\chi_i = 1$ for all $i = 1, 2, \ldots, N = J$; and moreover, if $\mathcal{P} = \mathcal{W}_\gamma$, then the crystalline curvature is 1.

Crystalline curvature flow. The normal velocity on $\mathcal{S}_i$ is $V_i = dh_i/dt$. Then the gradient flow of $\mathcal{E}_\gamma$ is $V = -\operatorname{grad}\mathcal{E}_\gamma[h]$, i.e.,

$$V_i = -\Lambda_\gamma(\boldsymbol{n}_i), \quad i = 1, 2, \ldots, N.$$

Note: To handle the gradient flow of $\mathcal{E}_\gamma$ (2.1) in the case where γ is a crystalline, we restricted smooth curve to admissible curve and introduced the crystalline curvature defined on each edge. This strategy was proposed by Taylor [34, 36, 35, 37] and independently by Angenent and Gurtin [3]. Also one can find essentially the same method as a numerical scheme for curvature flow equation in Roberts [31]. We refer the reader Almgren and Taylor [1] for detailed history. In the physical context, the region enclosed by $\mathcal{P}$ represents the crystal. See also Taylor, Cahn and Handwerker [38] and Gurtin [18] for physical background. Besides this crystalline strategy, other strategies by subdifferential and level-set method have been extensively studied. See Giga [9, 10, 11] and references theirin.

An area-preserving motion by crystalline curvature. The enclosed area $\mathcal{A}$ of $\mathcal{P}$ is given by

$$\mathcal{A}[h] = \frac{1}{2}\sum_{i=1}^{N} h_i d_i[h].$$

Then the rate of variation of $\mathcal{A}[h]$ in the direction φ is

$$\frac{\delta\mathcal{A}[h]}{\delta\varphi} = \frac{d}{d\varepsilon}\mathcal{A}[h+\varphi]\bigg|_{\varepsilon=0} = \sum_{i=1}^{N}\varphi_i d_i[h].$$

By taking $\varphi_i = -\left(\dfrac{\delta\mathcal{E}_\gamma[h]}{\delta h}\right)_i = -\Lambda_\gamma(\boldsymbol{n}_i)$, we have $\dfrac{\delta\mathcal{A}[h]}{\delta\varphi} = -\displaystyle\sum_{i=1}^{N}\Lambda_\gamma(\boldsymbol{n}_i)d_i[h]$. Hence by taking $\varphi_i = \overline{\Lambda}_\gamma - \Lambda_\gamma(\boldsymbol{n}_i)$, we have $\dfrac{\delta\mathcal{A}[h]}{\delta\varphi} = 0$. Here

$$\overline{\Lambda}_\gamma = \frac{\sum_{i=1}^{N}\Lambda_\gamma(\boldsymbol{n}_i)d_i[h]}{\sum_{k=1}^{N} d_k} = \frac{\sum_{i=1}^{N}\chi_i l_\gamma(\boldsymbol{n}_i)}{\mathcal{L}}$$

is the average of the crystalline curvature. Thus we have the gradient flow of $\mathcal{E}_\gamma$ along $\mathcal{P}$ which encloses a fixed area:

$$V_i = \overline{\Lambda}_\gamma - \Lambda_\gamma(\boldsymbol{n}_i), \quad i = 1, 2, \ldots, N. \tag{4.3}$$

In (4.3), $V_i = \dot{h}_i$ is the normal velocity on $\mathcal{S}_i$ in the direction $\boldsymbol{n}_i$. From (4.1), we have

$$\dot{d}_i = -(\cot\vartheta_i + \cot\vartheta_{i+1})V_i + V_{i-1}\operatorname{cosec}\vartheta_i + V_{i+1}\operatorname{cosec}\vartheta_{i+1}, \quad i = 1, 2, \ldots, N. \tag{4.4}$$

Furthermore, by (4.2) we have

$$\dot{\boldsymbol{p}}_i = V_i \boldsymbol{n}_i + \frac{V_{i-1} - (\boldsymbol{n}_{i-1} \cdot \boldsymbol{n}_i) V_i}{(\boldsymbol{n}_{i-1} \cdot \boldsymbol{t}_i)} \boldsymbol{t}_i, \quad i = 1, 2, \ldots, N. \tag{4.5}$$

Note that (4.3), (4.4) and (4.5) are equivalent each other.

Exercise 16 The time derivative of $\mathcal{E}_\gamma = \mathcal{E}_\gamma(t)$ and $\mathcal{A} = \mathcal{A}(t)$ are given by the following equations, respectively:

$$\frac{d}{dt}\mathcal{E}_\gamma(t) = \left.\frac{\delta \mathcal{E}_\gamma[h]}{\delta \varphi}\right|_{\varphi = \dot{h}} = \sum_{i=1}^{n} \Lambda_\gamma(\boldsymbol{n}_i) \dot{h}_i d_i = \sum_{i=1}^{n} \Lambda_\gamma(\boldsymbol{n}_i) V_i d_i,$$
$$\frac{d}{dt}\mathcal{A}(t) = \left.\frac{\delta \mathcal{A}[h]}{\delta \varphi}\right|_{\varphi = \dot{h}} = \sum_{i=1}^{n} \dot{h}_i d_i = \sum_{i=1}^{n} V_i d_i.$$

Check the following two basic properties:

$$\frac{d}{dt}\mathcal{E}_\gamma(t) \leq 0 \quad \text{and} \quad \frac{d}{dt}\mathcal{A}(t) = 0,$$

in the case where $V_i = \overline{\Lambda}_\gamma - \Lambda_\gamma(\boldsymbol{n}_i)$.

Problem. For a given essentially admissible closed curve $\mathcal{P}_0$, find a family of essentially admissible curves $\{P(t)\}_{0 \leq t < T}$ satisfying (4.3) (or (4.4) or (4.5)) with $\mathcal{P}(0) = \mathcal{P}_0$. Since (4.4) are the system of ordinary differential equations, the maximal existence time is positive: $T > 0$.

Question. What might happen to $\mathcal{P}(t)$ as t tends to $T \leq \infty$?

Known results and open problems. See the paragraph of Numerical simulations behind Procedure B in the next section.

5 Numerical scheme

The aims are to construct a numerical scheme which enjoys two basic properties $d\mathcal{E}_\gamma(t)/dt \leq 0$ and $d\mathcal{A}(t)/dt = 0$ (see Exercise 16), and to investigate what might happen to solution $\mathcal{P}(t)$ of the evolution equation (4.3) as t tends to $T \leq \infty$. We discretize the system of ordinary equations (4.3) or (4.4) or (4.5) with the initial essentially admissible closed curve $\mathcal{P}^0 = \mathcal{P}_0$ at the time $t_0 = 0$. Let $m = 0, 1, 2, \ldots$ be a step number. By a^m, we denote the approximation of $a(t_m)$ at the time $t_m = \sum_{i=0}^{m-1} \tau_i$ (the time step τ_m will be defined in the following procedure).

Procedure A (extension of [40]) Fix parameters $\mu \in [0, 1]$ and $\lambda, \varepsilon \in (0, 1)$. For a given essentially admissible N-sided closed curve $\mathcal{P}^m = \bigcup_{i=1}^{N} [\boldsymbol{p}_i^m, \boldsymbol{p}_{i+1}^m]$, we define $\mathcal{P}^{m+1} = \bigcup_{i=1}^{N} [\boldsymbol{p}_i^{m+1}, \boldsymbol{p}_{i+1}^{m+1}]$ as follows:

(i) the i-th length: $d_i^m = |\boldsymbol{p}_{i+1}^m - \boldsymbol{p}_i^m|$ $(\forall i)$;

(ii) the m-th variable time step: $\tau_m = \rho(d_{\min}^m)^2/\Delta$, where
$\rho = \varepsilon(1-\mu\lambda)\min\{\lambda, 1-\mu\lambda\}$, $\Delta = 2|\chi l_\gamma(\boldsymbol{n})|_{\max}(2/|\sin\vartheta|_{\min} + |\tan(\vartheta/2)|_{\max})$;

(iii) the i-th length d_i^{m+1}:
$(D_\tau d)_i^m = -(\cot\vartheta_i + \cot\vartheta_{i+1})V_i^{m+\mu} + V_{i-1}^{m+\mu}\operatorname{cosec}\vartheta_i + V_{i+1}^{m+\mu}\operatorname{cosec}\vartheta_{i+1}$ $(\forall i)$;

(iv) the i-th hight h_i^{m+1}: $(D_\tau h)_i^m = V_i^{m+\mu}$ $(\forall i)$;

(v) the i-th vertex: $\boldsymbol{p}_i^{m+1} = h_i^{m+1}\boldsymbol{n}_i + \dfrac{h_{i-1}^{m+1} - (\boldsymbol{n}_{i-1}\cdot\boldsymbol{n}_i)h_i^{m+1}}{\boldsymbol{n}_{i-1}\cdot\boldsymbol{t}_i}\boldsymbol{t}_i$ $(\forall i)$;

(vi) the new time: $t_{m+1} = t_m + \tau_m$.

Here we have used the notation: $a_{\min} = \min_i a_i$, $|a|_{\min} = \min_i |a_i|$, $|a|_{\max} = \max_i |a_i|$, and $(D_\tau a)_i^m = (a_i^{m+1} - a_i^m)/\tau_m$.

Two basic properties. One is that the total energy $\mathcal{E}_\gamma^m$ is decreasing in steps: $(D_\tau \mathcal{E}_\gamma)^m \le 0$ for any $\mu \in [0,1]$. The other is that the area enclosed by $\mathcal{P}^m$, say $\mathcal{A}^m$, is preserved: $(D_\tau \mathcal{A})^m = 0$ if $\mu = 1/2$.

Iteration. In (iii), if $\mu \in (0,1]$, we solve the following iteration starting from $z_i^0 = d_i^m$:

$$\frac{z_i^{k+1} - z_i^0}{\tau_m} = -(\cot\vartheta_i + \cot\vartheta_{i+1})\widetilde{V}_i^{m+\mu} + \widetilde{V}_{i-1}^{m+\mu}\operatorname{cosec}\vartheta_i + \widetilde{V}_{i+1}^{m+\mu}\operatorname{cosec}\vartheta_{i+1},$$
$$\widetilde{V}_i^{m+\mu} = \frac{\chi_i l_\gamma(\boldsymbol{n}_i)}{\widetilde{d}_i^{m+\mu}} - \frac{\sum_{j=1}^N \chi_j l_\gamma(\boldsymbol{n}_j)}{\sum_{k=1}^N \widetilde{d}_k^{m+\mu}}, \quad \widetilde{d}_i^{m+\mu} = (1-\mu)z_i^0 + \mu z_i^k, \quad k = 0, 1, \dots$$

Convergence $\lim_{k\to\infty} z_i^k = d_i^{m+1}$ and positivity $d_i^{m+1} \ge (1-\lambda)d_i^m > 0$ hold for all i ([40]).

The maximal existence time. Since the above positivity $d_i^m > 0$ holds, we can keep iterating Procedure A in finitely many steps (even if $\mathcal{P}^m$ self-intersects at a step m, we can continue). Then the maximal existence time is $t_\infty = \lim_{m\to\infty}\sum_{k=0}^m \tau_k$. Here we have two questions: one is whether t_∞ is finite or not, and the other is what might happen to $\mathcal{P}^m$ as m tends to infinity. It is known that $t_\infty = \infty$ holds if W_γ is an N-sided regular polygon and $\mathcal{P}^0$ is an admissible convex polygon ([40]).

Extension. At the maximal existence time t_∞, it is possible that at least one edge, say the i-th edge, may disappear. If $\chi_i = 0$ or $l_\gamma(\boldsymbol{n}_i) = 0$, then $\mathcal{P}^\infty$ is still essentially admissible. Hence we can continue Procedure A starting from the initial curve $\mathcal{P}^\infty$. In practice, if some edges are small enough, we eliminate them artificially as the following procedure.

Procedure B Put a positive parameter $\delta \ll 1$. For every step m, do the followings:

(i) define $D = \min\{d_i^m \,|\, \chi_i \ne 0,\ l_\gamma(\boldsymbol{n}_i) > 0\}$ (this is well-defined);

(ii) find the value k such that $d_k^m = \min\{d_i^m \,|\, \chi_i = 0\}$ (if it exists);
find the value j such that $d_j^m = \min\{d_i^m \,|\, \chi_i \neq 0,\ l_\gamma(\boldsymbol{n}_i) = 0\}$ (if it exists);

(iii) if k or j exists, check the followings:
(a) if $d_k^m/D < \delta$ and if $d_k^m \leq d_j^m$ or the value j does not exist, then eliminate the k-th edge (see Figure 16 (left));
(b) if $d_j^m/D < \delta$ and if $d_j^m < d_k^m$ or the value k does not exist, then eliminate the j-th edge (see Figure 16 (right));
(c) otherwise, exit from Procedure B;

(iv) in (iii), if (a) occurred, then do renumbering within the new number $N := N - 2$;
else if (b) occurred, then do renumbering within the new number $N := N - 1$.

Numerical computation will be continued repeating Procedure A and B.

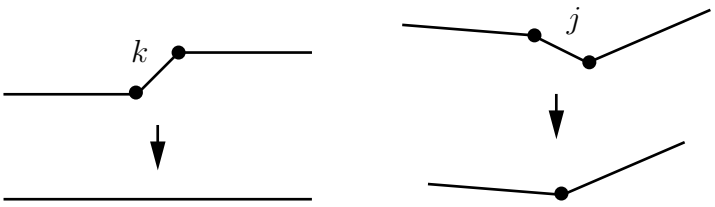

Figure 16: Two types of elimination of some edges in Procedure B (iii). (Left): In the type of (iii) (a), the number of particles decreases from N to $N - 2$. (Right)): In the type of (iii) (b), the number of particles decreases from N to $N - 1$.

Numerical simulations. In the following five figures on each line, from left to right, they indicate W_γ, $\mathcal{P}^0$, $\mathcal{P}^{m_1}$, $\mathcal{P}^{m_2}$, $\mathcal{P}^{m_3}$ $(0 < m_1 < m_2 < m_3)$.

The case where $\boldsymbol{\mathcal{P}_0}$ is convex and admissible. The solution polygon $\mathcal{P}(t)$ exists globally in time, and $\mathcal{P}(t)$ converges to W_γ as t tends to infinity. See Yazaki [43] in the case $\gamma = const.$, and Yazaki [44, PartI] in general. See also Gage [6] for the smooth case. On the convergence between $\Gamma(t_m)$ and $\mathcal{P}(t_m)$, see Ushijima and Yazaki [40].

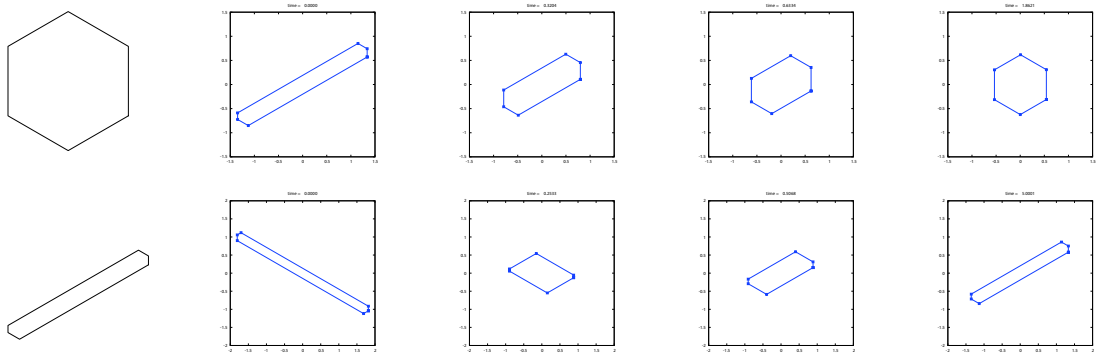

The case where $\mathcal{P}_0$ is convex and essentially admissible. By a similar proof as in Yazaki [43] or Yazaki [45], it can be proved that if the maximal existence time $T < \infty$ and the i-th edge disappears as t tends to T, then $l_\gamma(\boldsymbol{n}_i) = 0$. That is, the normal vector of vanishing edge does not belong to $\mathcal{N}_\gamma$, and $\inf_{0<t<T}\{d_i(t) \,|\, l_\gamma(\boldsymbol{n}_i) > 0\} > 0$ holds.

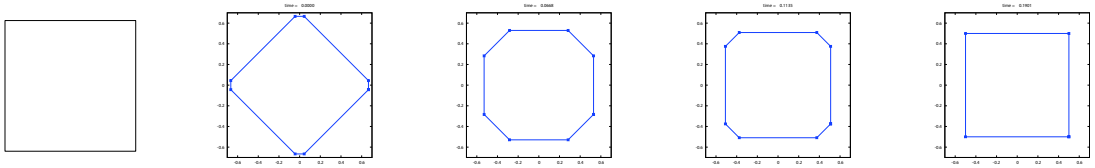

Open Problems: For any essentially admissible convex polygon $\mathcal{P}_0$, is T a finite value? This is still open. If the answer of this question is yes, then we have the finite time sequence $T_1 < T_2 < \cdots < T_M$ such that $\mathcal{P}(T_i)$ is essentially admissible for $i = 1, 2, \ldots, M-1$ and $\mathcal{P}(T_M)$ is admissible. In the general case where $V_i = g(\boldsymbol{n}_i, \Lambda_\gamma(\boldsymbol{n}_i))$ with the condition $g > 0$, the answer of the above question is yes. See Yazaki [45]. Note that g does not include $\overline{\Lambda}_\gamma$.

The case where $\mathcal{P}_0$ is nonconvex and admissible. The following figure indicates convexified phenomena.

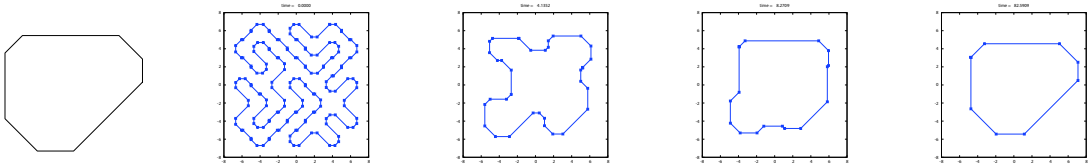

In smooth case, a self-intersection is conjectured in Gage [6], and is proved in Mayer and Simonett [30]. The following figure is a numerical example of self-intersection.

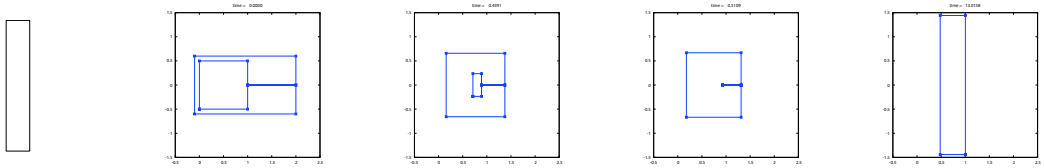

Open Problems: At this stage, we have the following three open problems:

(1) Does $\mathcal{P}(t)$ become convex in finite time?

(2) Will the admissibility be preserved?

(3) Does $\mathcal{P}(t)$ self-intersect?

We have information related to these three questions. (1) In the case where $V_i = -\gamma(\boldsymbol{n}_i)|\Lambda_\gamma(\boldsymbol{n}_i)|^{\alpha-1}\Lambda_\gamma(\boldsymbol{n}_i)$, there exist $\alpha \in (0,1)$, γ and $\mathcal{P}_0$ such that nonconvex solution curve $\mathcal{P}(t)$ shrinks homothetically, i.e., there exists a nonconvex self-similar solution polygonal curve. See Ishiwata, Ushijima, Yagisita and Yazaki [26]. (2) In the case where

$V_i = -a(\boldsymbol{n}_i)|\Lambda_\gamma(\boldsymbol{n}_i)|^{\alpha-1}\Lambda_\gamma(\boldsymbol{n}_i)$, for any $\alpha \geq 1$, $a(\cdot)$ and $\mathcal{P}_0$ if γ is symmetric, then the solution curve keeps admissibility. See Giga and Giga [12]. However, there exist $\alpha \in (0,1)$, $a(\cdot)$ and $\mathcal{P}_0$ such that the admissibility collapses in finite time, i.e., we have the examples that admissible nonconvex polygonal curve becomes nonadmissible in finite time. See Hirota, Ishiwata and Yazaki [20, 21]. (3) The above figure indicates the possibility of self-intersection.

References

[1] F. Almgren and J. E. Taylor, *Flat flow is motion by crystalline curvature for curves with crystalline energies*, J. Diff. Geom. **42** (1995) 1–22.

[2] B. Andrews, *Singularities in crystalline curvature flows*, Asian J. Math. **6** (2002) 101–122.

[3] S. Angenent and M. E. Gurtin, *Multiphase thermomechanics with interfacial structure, 2. Evolution of an isothermal interface*, Arch. Rational Mech. Anal. **108** (1989) 323–391.

[4] S. Angenent and J. J. L Velázquez, *Asymptotic shape of cusp singularities in curve shortening*, Duke Math. J. **77** (1995) 71–110.

[5] K.-S. Chou and X.-P. Zhu, *A convexity theorem for a class of anisotropic flows of plane curves*, Indiana Univ. Math. J. **48** (1999) 139–154.

[6] M. Gage, *On an area-preserving evolution equations for plane curves*, Contemporary Math. **51** (1986) 51–62.

[7] M. Gage and R. S. Hamilton, *The heat equation shrinking convex plane curves*, J. Diff. Geom. **23** (1986) 69–96.

[8] Y. Giga, *A level set method for surface evolution equations*, Sūgaku **47** (1995) 321–340; English transl., Sugaku Expositions **10** (1997) 217–241.

[9] Y. Giga, *Interesting diffusion equations*, Sūgaku **49** (1997) 193–196. (Japanese)

[10] Y. Giga, *Interface dynamics — effects of curvature*, Hokkaido University Technical Report Series **56** (1998). (Japanese)

[11] Y. Giga, *Anisotropic curvature effects in interface dynamics*, Sūgaku **52** (2000) 113–127; English transl., Sugaku Expositions **16** (2003) 135–152.

[12] M.-H. Giga and Y. Giga, *Crystalline and level set flow – convergence of a crystalline algorithm for a general anisotropic curvature flow in the plane*, Free boundary problems: theory and applications, I (Chiba, 1999), GAKUTO Internat. Ser. Math. Sci. Appl., Gakkōtosho, Tokyo **13** (2000) 64–79.

[13] M.-H. Giga, Y. Giga and H. Hontani, *Self-similar expanding solutions in a sector for a crystalline flow*, SIAM J. Math. Anal. **37** (2006) 1207–1226.

[14] Y. Giga and M. E. Gurtin, *A comparison theorem for crystalline evolution in the plane*, Quart. J. Appl. Math. **LIV** (1996) 727–737.

[15] Y. Giga and K. Yama-uchi , *On a lower bound for the extinction time of surfaces moved by mean curvature*, Calc. Var. **1** (1993) 417–428.

[16] P. M. Girão, *Convergence of a crystalline algorithm for the motion of a simple closed convex curve by weighted curvature*, SIAM J. Numer. Anal. **32** (1995) 886–899.

[17] M. A. Grayson, *The heat equation shrinks emmbedded plane curves to round points*, J. Diff. Geom. **26** (1987) 285–314.

[18] M. E. Gurtin, *Thermomechanics of evolving phase boundaries in the plane*, Oxford, Clarendon Press (1993).

[19] C. Hirota, T. Ishiwata and S. Yazaki, *Some results on singularities of solutions to an anisotropic crystalline curvature flow*, Proceedings of the Third Polish-Japanese Days (Chiba, 2004), GAKUTO Internat. Ser. Math. Sci. Appl., Gakkōtosho, Tokyo **23** (2005) 119–128.

[20] C. Hirota, T. Ishiwata and S. Yazaki, *Note on the asymptotic behavior of solutions to an anisotropic crystalline curvature flow*, Recent Advances on Elliptic and Parabolic Issues (Editors: Michel Chipot and Hirokazu Ninomiya), Proceedings of the 2004 Swiss-Japan Seminar, World Scientific (2006) 129–143.

[21] C. Hirota, T. Ishiwata and S. Yazaki, *Numerical study and examples on singularities of solutions to anisotropic crystalline curvature flows of nonconvex polygonal curves*, Advanced Studies in Pure Mathematics (ASPM); Proceedings of MSJ-IRI 2005 "Asymptotic Analysis and Singularity" (Sendai, 2005) (to appear).

[22] H. Hontani, M.-H. Giga, Y. Giga and K. Deguchi, *Expanding selfsimilar solutions of a crystalline flow with applications to contour figure analysis*, Discrete Applied Mathematics **147** (2005) 265–285.

[23] H. Ishii , G. E. Pires and P. E. Souganidis, *Threshold dynamics type approximation schemes for propagating fronts*, J. Maht. Soc, Japan **51** (1999) 267–308.

[24] K. Ishii and H. M. Soner , *Regularity and convergence of crystalline motion*, SIAM J. Math. Anal. **30** (1999) 19–37.

[25] T. Ishiwata , T. K. Ushijima and S. Yazaki, *An eigenvalue problem of the second order difference approximation in a crystalline setting*, in preparation.

[26] T. Ishiwata , T. K. Ushijima , H. Yagisita and S. Yazaki, *Two examples of nonconvex self-similar solution curves for a crystalline curvature flow*, Proc. Japan Academy **80**, Ser. A, No. 8 (2004) 151–154.

[27] T. Ishiwata and S. Yazaki, *On the blow-up rate for fast blow-up solutions arising in an anisotropic crystalline motion*, J. Comp. App. Math. **159** (2003) 55–64.

[28] T. Ishiwata and S. Yazaki, *A fast blow-up solution and degenerate pinching arising in an anisotropic crystalline motion*, submitted.

[29] R. Kobayashi and Y. Giga, *On anisotropy and curvature effects for growing crystals*, Japan J. Indust. Appl. Math. **18** (2001) 207–230.

[30] U. F. Mayer and G. Simonett, *Self-intersections for the surface diffusion and the volume-preserving mean curvature flow*, Differential Integral Equations **13** (2000) 1189–1199.

[31] S. Roberts, *A line element algorithm for curve flow problems in the plane*, CMA Research Report **58** (1989); J. Austral. Math. Soc. Ser. B **35** (1993) 244–261.

[32] J. A. Sethian, *Level set methods: evolving interfaces in geometry, fluid mechanics, computer vision, and materials science*, Cambridge Monographs on Applied and Computational Mathematics **3**, Cambridge University Press, Cambridge (1996).

[33] A. Stancu, *Uniqueness of self-similar solutions for a crystalline flow*, Indiana Univ. Math. J. **45** (1996) 1157–1174.

[34] J. E. Taylor, *Crystals, in equilibrium and otherwise*, videotape of 1989 AMS-MAA lecture, Selected Lectures in Math., Amer. Math. Soc. (1990).

[35] J. E. Taylor, *Constructions and conjectures in crystalline nondifferential geometry*, Proceedings of the Conference on Differential Geometry, Rio de Janeiro, Pitman Monographs Surveys Pure Appl. Math. **52** (1991) 321–336, Pitman London.

[36] J. E. Taylor, *Motion by crystalline curvature*, Computing Optimal Geometries, Selected Lectures in Math., Amer. Math. Soc. (1991) 63–65 plus video.

[37] J. E. Taylor, *Motion of curves by crystalline curvature, including triple junctions and boundary points*, Diff. Geom.: partial diff. eqs. on manifolds (Los Angeles, CA, 1990), Proc. Sympos. Pure Math., **54** (1993), Part I, 417–438, AMS, Providencd, RI.

[38] J. E. Taylor, J. Cahn and C. Handwerker, *Geometric models of crystal growth*, Acta Metall., **40** (1992) 1443–1474.

[39] T. K. Ushijima and S. Yazaki, *Convergence of a crystalline algorithm for the motion of a closed convex curve by a power of curvature $V = K^{\alpha}$*, SIAM Journal on Numerical Analysis **37** (2000) 500–522.

[40] T. K. Ushijima and S. Yazaki, *Convergence of a crystalline approximation for an area-preserving motion*, Journal of Computational and Applied Mathematics **166** (2004) 427–452.

[41] S. Yazaki, *Point-extinction and geometric expansion of solutions to a crystalline motion*, Hokkaido Math. J. **30** (2001) 327–357.

[42] S. Yazaki, *Asymptotic behavior of solutions to an expanding motion by a negative power of crystalline curvature*, Adv. Math. Sci. Appl. **12** (2002) 227–243.

[43] S. Yazaki, *On an area-preserving crystalline motion*, Calc. Var. **14** (2002) 85–105.

[44] S. Yazaki, *On an anisotropic area-preserving crystalline motion and motion of nonadmissible polygons by crystalline curvature*, Sūrikaisekikenkyūsho Kōkyūroku **1356** (2004) 44–58.

[45] S. Yazaki, *Motion of nonadmissible convex polygons by crystalline curvature*, Publications of Research Institute for Mathematical Sciences (to appear).